JACS
JOURNAL OF THE AMERICAN CHEMICAL SOCIETY
Article
pubs.acs.org/JACS

It Is the Outside That Counts: Chemical and Physical Control of Dynamic Surfaces

Sarah M. Brosnan, Andrew H. Brown, and Valerie Sheares Ashby*

Department of Chemistry, University of North Carolina at Chapel Hill, 131 South Road, Chapel Hill, North Carolina 27510-3290, United States

Supporting Information

ABSTRACT: Materials capable of dynamically controlling surface chemistry and topography are highly desirable. We have designed a system that is uniquely able to remotely control the presented functionality and geometry at a given time by using a functionalizable shape memory material. This was accomplished by incorporating controlled amounts of an azide-containing monomer into a shape memory polymeric material. These materials are capable of physically changing surface geometry over a broad range of length scales from >1 mm to 100 nm. Using copper-assisted click chemistry, they can be functionalized with a variety of molecules to yield different surfaces. Combining these features gave materials that can change both the presented geometry and functionality at tunable transition temperatures.

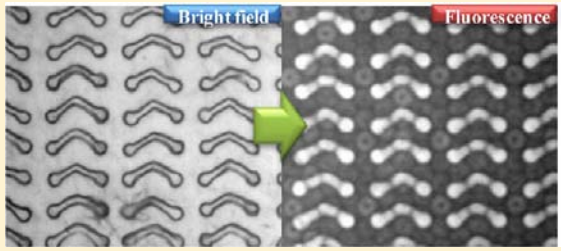

INTRODUCTION

Controllable surface properties, such as surface energy and topography, are extremely desirable. How a material interfaces with its environment is fundamental to its function; thus, research into the development of such materials has been extensive.[1−6] This is especially important for biomaterials, as surface energy and topography affect critical properties such as biocompatibility; cell growth, adhesion, alignment, and differentiation; biodegradation; and protein absorption. Dynamic control of these functions is even more attractive. Applications for such dynamic materials range from deployable materials (such as stents)[7−9] to simulation of in vivo environments (cell signaling events)[10] and biosensors.[11]

Stimuli responsive materials have long been aimed to meet these goals.[12−16] Temperature and pH-responsive hydrogels, such as poly(*N*-isopropylacrylamide) and its copolymers, have shown to be good actuating cell substrates, as they can switch between hydrophilic and hydrophobic surface depending on temperature (above or below its LCST).[17−21] Shape memory polymeric (SMPs) materials as dynamic substrates have also been recently explored.[22−24] These materials are programmed from one shape to another, with the application of heat and force, and they remain in that temporary shape until heated above the transition temperature. These materials demonstrate excellent dynamic control of topography (SMPs) and hydrophilicity (hydrogels); however, the chemical structure of these materials limits their ability to be chemically surface-modified without the loss of their thermal and mechanical properties. Thus, a truly versatile material capable of tunable and dynamic surface chemistry and topography has remained elusive.

Herein, we describe the material development, surface functionalization, and dynamic surface switching behavior of a material that enables true control of both its surface chemistry and topography. This was accomplished by designing a shape memory thermoset that contained a known shape memory polymer, poly(octylene adipate), and a novel and easily functionalizable polymer, poly(octylene diazoadipate). Adjusting the ratios of the two segments allowed for facile control of the transition temperature. Topographical actuation on multiple length scales (1 mm to 100 nm) was easily achieved, and the surface of the material was easily functionalized with a variety of alkynes (e.g., hydrophilic to hydrophobic and reactive to nonreactive) using copper-assisted Huisgen [3 + 2]-cycloaddition (click chemistry). The combination of micro- and nanoscopic shape memory with surface functionalization produced materials that could tunably switch both their surface chemistry and topography as they transitioned through the shape memory cycle. These materials are therefore ideal substrates for scenarios in which control of the surface chemistry and topography is critical.

RESULTS AND DISCUSSION

Material Development. Scheme 1 outlines the synthetic strategy chosen for the preparation of the dynamic substrates. The base material is a semicrystalline polyester which allowed for control of monomer ratios, molecular weights, end groups, and melting transition temperatures (i.e., switching temperature). To ensure mild reaction conditions for surface modification, azides were incorporated into the main polymer chain, with the intent of utilizing the copper-assisted click chemistry.[25−29] Click chemistry is favorable for biological

Received: September 10, 2012
Published: January 15, 2013

   dx.doi.org/10.1021/ja308080g | J. Am. Chem. Soc. 2013, 135, 3067−3072

Scheme 1. Synthesis of Azide-Containing Shape Memory Thermosets

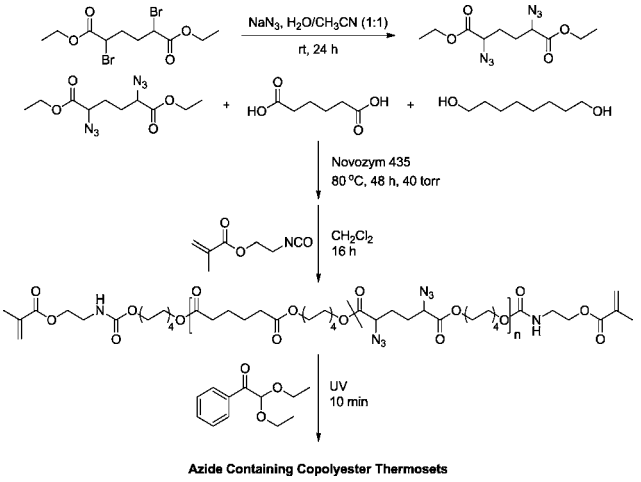

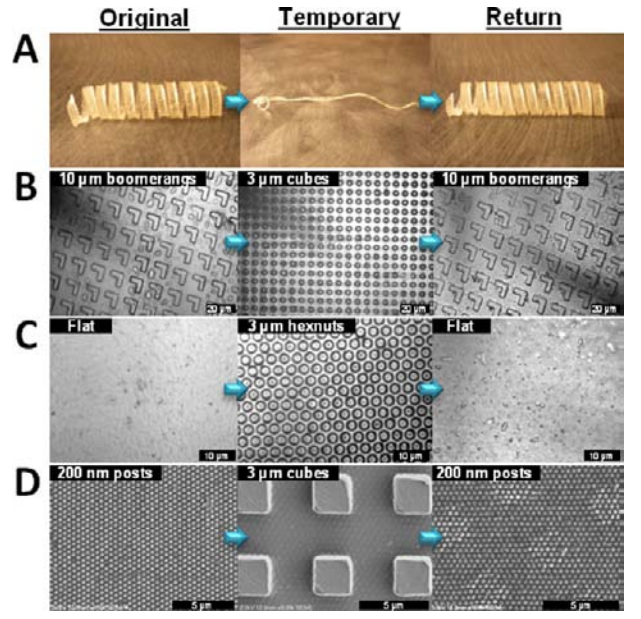

Figure 1. Macro-, micro-, and nanoscopic shape memory cycles. (A) The macroscopic transition is a curly film (3 cm in length) that has been placed into a straight secondary shape and is able to recover to the curly shape upon heating above its melting transition. The micro- and nanoscopic shape transitions show (B) 10 × 1 μm boomerang shapes to 3 × 3 × 3 μm cubes and then back to boomerangs, (C) flat to 3 × 1 μm hexnuts and then return to the flat film, and (D) SEM of transition from 200 nm posts to 3 × 3 × 3 μm and then back to 200 nm posts. The residual cube shape is less than hundreds of nanometers in height, demonstrating a near complete transition.

applications due to the general biocompatibility of many alkynes and azides, the ease of monomer synthesis, and the extensive library of commercially available alkynes. While there are other examples of azide-containing polyesters in the literature,[30−32] this synthetic route allowed for easy and safe fine-tuning of the melting temperature between 27 °C to 64 °C through incorporation of the diazide monomer from 0% to 38 mol %, respectively (Table S1, Supporting Information). For consistency, the formulation with 19 mol % of diazide monomer, melting temperature of 38 °C, was used for this study.

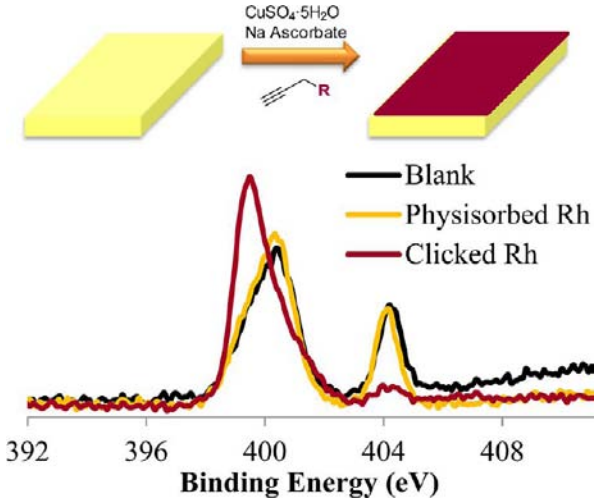

Figure 2. The top panel shows the scheme for the surface functionalization of the shape memory materials. The bottom panel shows the XPS results for the blank, physisorbed, and clicked samples (alkyne-functionalized Rhodamine B). The *y*-axis (not shown) represents intensity (cps, counts per second). The absence of the peak at 404 eV and the shift of the 400 eV peak indicate that the azides reacted to give the triazole product (curve-fitting analysis is in the Supporting Information).

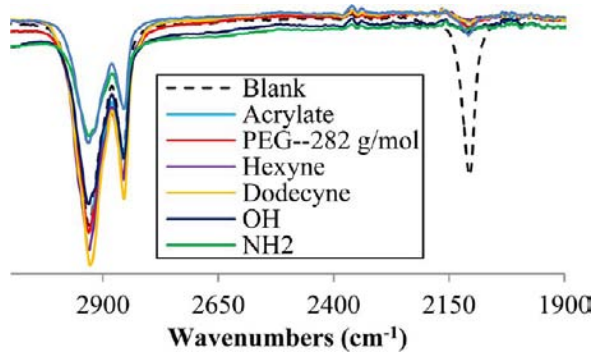

Figure 3. ATR-FTIR spectra of the blank and functionalized films. The decrease in signal at 2100 cm^{-1} indicates that the azide functionality has been reacted. Full spectra of both modified flat and hexnut surfaces are shown in the Supporting Information.

The shape memory ability of these materials was first analyzed by the macroscopic shape memory performance (deformations ≥1 mm) of the polymers. This performance was quantified by determining the strain fixity ratio, R_f, and the strain recovery ratio, R_r, which measures how well the polymer fixes the temporary shape and then returns to its original shape, respectively. Very good shape memory properties, indicated by R_f and R_r values greater than 95%, were observed with copolymers that had diazide monomer incorporation between 0% and 30% (Table S2, Supporting Information). The results illustrated in Figure 1 show images of a material undergoing a transition from its curled primary shape to a straight secondary and back to the curled primary shape.

To have precisely defined surface features, for shape memory on the micro- and nanoscales, PRINT (Particle Replication in Nonwetting Templates) molds were utilized. PRINT is normally used to make monodisperse particles of varying size and shape, but here the molds were used to surface emboss a range of precisely defined, high fidelity shapes (such as cubes,

dx.doi.org/10.1021/ja308080g | J. Am. Chem. Soc. 2013, 135, 3067−3072

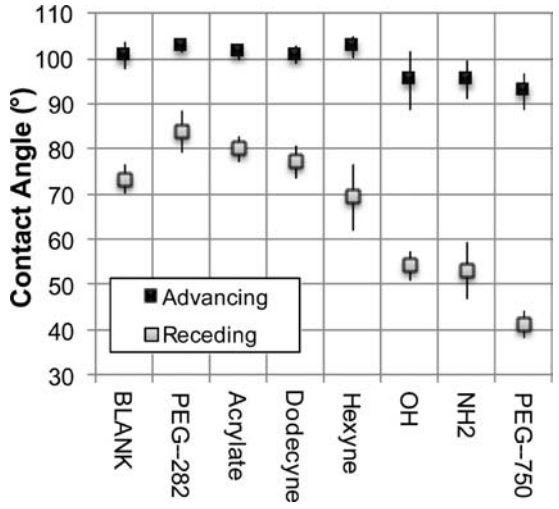

Figure 4. Dynamic contact angle data for the blank and functionalized films. The difference in hystereses for the different attached functionalities indicates that we have indeed made different surfaces.

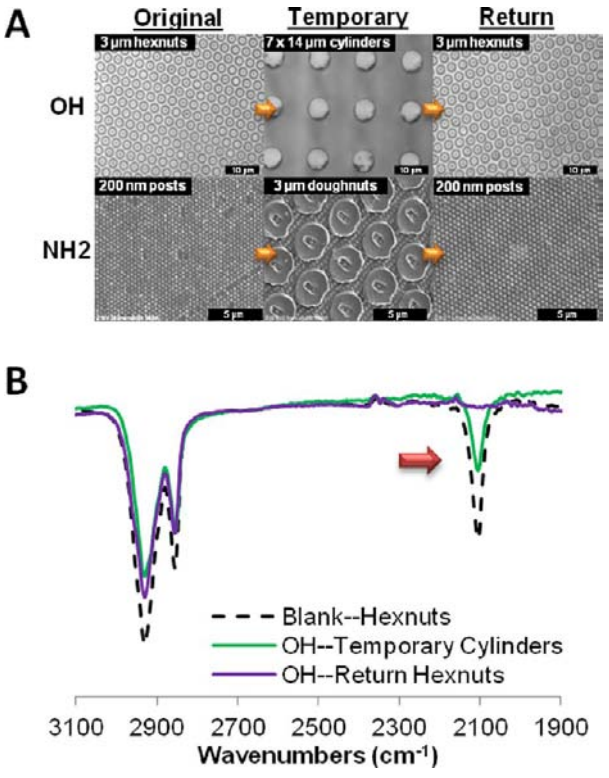

Figure 5. Functionalized films through shape memory cycles. (A) Top image shows the transition from 3 × 1 μm hexnuts (modified with propargyl alcohol) to 7 × 14 μm cylinders and then back to 3 × 1 μm hexnuts. Bottom image shows 200 nm posts (modified with propargylamine) to 3 μm doughnut shapes and then back to 200 nm posts. (B) ATR-FTIR spectra of the secondary and return shapes of a surface functionalized with propargyl alcohol compared to an unmodified hexnut embossed film, which shows the azides appearing and disappearing as the film goes through the shape memory cycle.

hexnuts, and cylinders) on the micro- and nanoscale (Scheme S1 illustrates the process of embossment). In Figure 1, the microscopic shape memory of these materials is demonstrated by their transition from small to large features, featured surfaces to nonfeatured surfaces, and large to small features. Nanoscopic

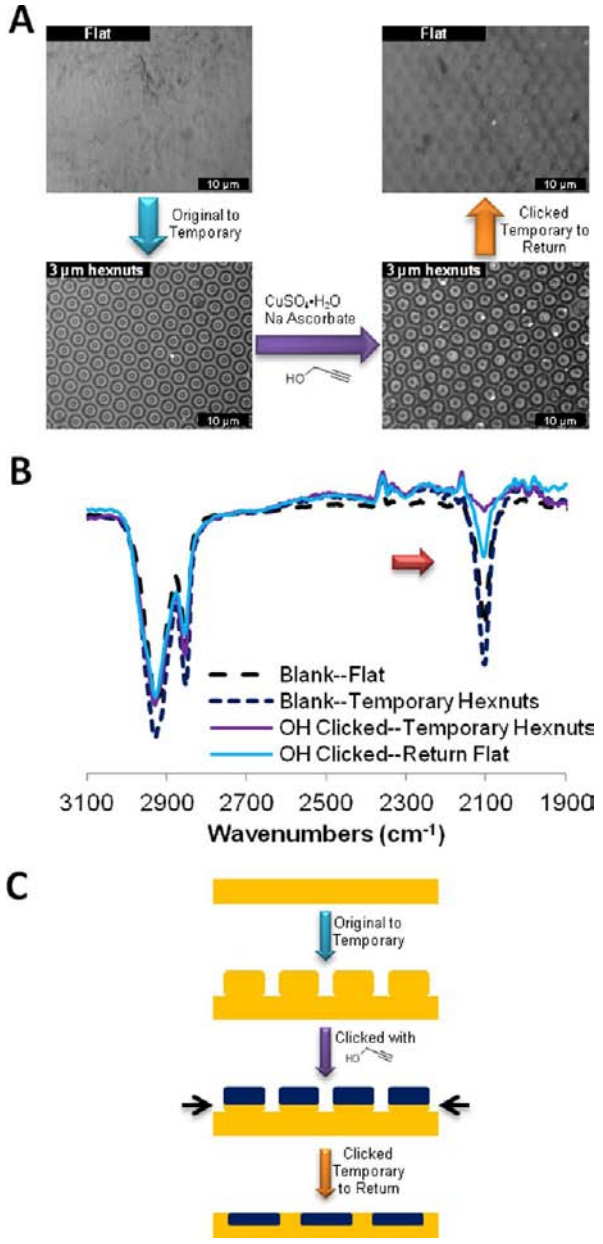

Figure 6. Functionalization at the temporary shape. (A) Microscopic images and scheme showing how the functionalization at the temporary shape was accomplished. (B) ATR-FTIR spectra showing that the azides are present before functionalization, disappear when clicked, and then reappear when the material is returned to its original shape. (C) Cartoon indicating where the functionalization, in blue, occurs and the extent of attenuation of the ATR-FTIR beam (shown with the black arrows).

shape memory was also achieved, as indicated by the ability to shift from 3 × 3 × 3 μm cubes to 200 nm posts.

Surface Functionalization. To first demonstrate the ability to chemically surface functionalize this azide-containing shape memory material an alkyne-modified Rhodamine B was used to modify the surface. The surface attachment was monitored by XPS at a penetration depth of 10 nm. Three flat samples were prepared: one with no functionalization (blank), one exposed to the same reaction conditions except the copper catalyst (physisorbed), and one chemically clicked sample (clicked). Azides have two peaks in the nitrogen 1s region of the spectrum, one at approximately 404 eV (specifically to

dx.doi.org/10.1021/ja308080g | J. Am. Chem. Soc. 2013, 135, 3067−3072

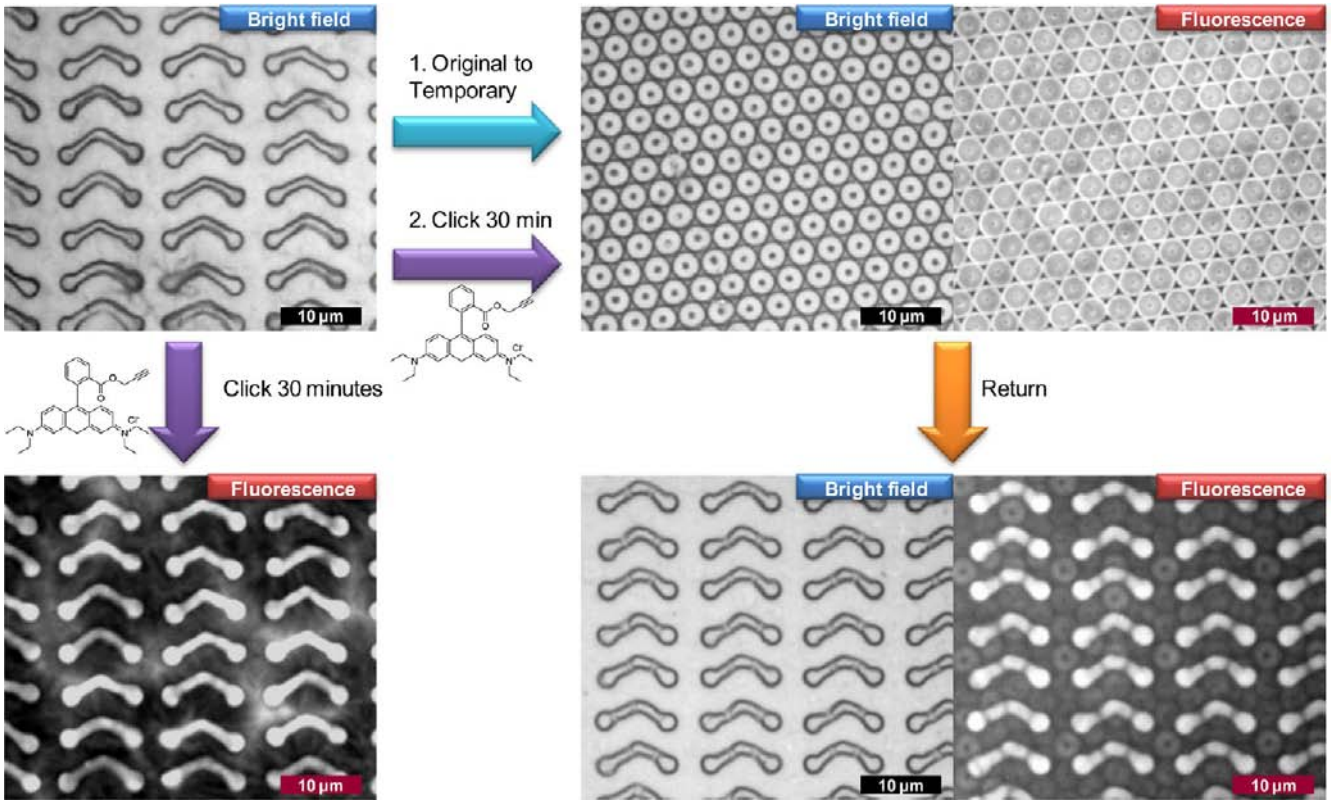

Figure 7. Clicking an alkyne-functionalized Rhodamine B for 30 min on a secondary 3 μm doughnuts shape. It is clear that the tops of the doughnut shapes are preferentially functionalized.

azides) and another at 397 eV (common to all nitrogens).[28] In Figure 2, the blank film (black) and physisorbed film (pink) spectra exhibit both nitrogen peaks. The right spectrum (clicked Rhodamine B film) exhibits the reduction or absence of the azide peak at 404 eV, which indicates that a click reaction has occurred, and the nitrogen shift to 399 eV, which corresponds to the appearance of the triazole. Another example of clicking 6-iodohexyne to the surface is shown in the Figure S6, Supporting Information.

The same method was then used to functionalize the surface with a variety of functional alkynes demonstrating tunability of the surface chemistry. To demonstrate the versatility of the system the following functional groups: hexyne, dodecyne, propargyl alcohol (OH), propargylamine (NH2), and 282 g/mol and 750 g/mol monoalkyne-functionalized poly(ethylene glycol) (PEG-282 and PEG-750) were covalently attached to the polymer film surface using click chemistry. It is important to emphasize, that these functionalities can be incorporated into a shape memory polymer without altering the thermal and mechanical properties, (Table S3, Supporting Information). These reactions were completed under mild conditions with patterned and nonpatterned surfaces. The extent of reaction was confirmed by the decrease of the azide antisymmetric stretch at 2100 cm^{-1} in ATR-FTIR spectra (Figure 3). ATR-FTIR has a penetration depth of only a few micrometers into a surface, so these data confirm that the surfaces were chemically altered.

The effect of the surface modifications on the wetting behavior was studied by dynamic contact angle measurements with flat substrates. As shown in Figure 4,the advancing contact angles of the more hydrophobic alkynes were similar to that of the blank substrate (without chemical attachment), while the more hydrophilic substrates were slightly lower, but they were still above 90°. This result demonstrates that the bulk material is fundamentally hydrophobic. The effect of the functionality is most profound when looking at the receding contact angles. Once again, the hydrophobic substrates have contact angles similar to those of the blank substrate; however, the effect on the highly hydrophilic functionalities is much more pronounced, with hysteresis between 40° and 50°. Hysteresis can be caused by many different phenomena, such as surface roughness, heterogeneity, reorientation, and swelling. All samples were made under the same conditions and have the same surface roughness, and there is a correlation between hydrophilicity and increased hysteresis. It is clear that the hysteresis in this case is caused by the rearrangement of the more hydrophilic surface groups.[33−36] This result shows that we have indeed produced surfaces that are significantly different from each other with the same polymer and functionalization technique.

Dynamic Surface Switching. To demonstrate the unique ability of our materials to switch their surface chemistry, films were functionalized at the primary shape and then taken through a shape memory transition (Figure 5). Using ATR-FTIR, it is clear that, at the initial shape, the films are surface functionalized (up to a few micrometers). When the films are in their temporary shape, however, some azides appear to have emerged on the surface, as shown in Figure 5B. This emergence is not entirely surprising because modification is predominantly a surface technique, and force is required to emboss the material into a secondary shape. The thickness of the film decreases as the total presented area increases, revealing new unreacted azides to the surface. The exceptional fidelity of the surface shape memory effect is further demonstrated when this

dx.doi.org/10.1021/ja308080g | J. Am. Chem. Soc. 2013, 135, 3067−3072

material returns to its original shape; the newly exposed azides disappear back into the bulk and are no longer visible by ATR-FTIR.

The reappearance of the azides on the surface invited the possibility of performing click reactions in the temporary state. These reactions produced rather interesting results, as shown in Figure 6. A flat film was deformed to produce a temporary 3 × 1 μm hexnut surface that was then chemically modified with propargyl alcohol. The temporary hexnuts were not greatly damaged by the click reaction, and the ATR-FTIR results show that the reaction was nearly complete. When the material was then returned to the flat original shape (now chemically modified with alcohol groups), it was apparent from the ATR-FTIR that there was an increase of azides on the surface. This is an interesting result because it demonstrates both the proximity of the functionality to the surface (within the attenuation of the ATR-FTIR beam) and the possibility of hiding functionalities on the surface by taking advantage of the presented surface area at a given time.

This selective functionalization hypothesis is supported by the experiment shown in Figure 7, where Rhodamine is reacted on the secondary shape for only 30 min. First, a boomerang primary shape is either functionalized for 30 min with an alkyne-functionalized Rhodamine B or is embossed with a secondary doughnut shape. The secondary doughnut shapes are then functionalized for 30 min. The functionalized doughnuts are then returned to the primary boomerang shapes. Because the reaction proceeds for such a small amount time, only the tops of the doughnuts are functionalized, and the doughnut shape can be seen on top of the boomerangs after returning to the primary shape. When these results are compared to the clicking of the primary shape, only the tops of the boomerangs show the Rhodamine functionality. These results are very exciting because they provide visual evidence for the above hypothesis; we can control the placement of functionality using the shape memory ability of these materials.

■ CONCLUSION

We have developed the first example of a truly multifunctional shape memory material, which has a broad impact on shape memory polymers and their applications. The designed material's shape memory transition can be adjusted (27 °C to 64 °C) by simply altering the copolymer ratio. In addition to exhibiting excellent shape memory properties on the macro-, micro-, and nanoscales, the surface chemistry of the material can be altered by functionalization with copper click chemistry. That is, this material is uniquely capable of adjusting its surface chemistry by simply clicking on the desired functionality at either the initial or temporary shape, thus creating a material that is capable of both geometric and chemical surface switching. These results are particularly exciting as cell-dictating substrates that can deliver a unique combination of physical and chemical cues at the will of the researcher.

■ ASSOCIATED CONTENT

Supporting Information

Experimental methods along with data for the prepolymer and cross-linked films, cytotoxicity data for the blank and functionalized films, full spectra of the ATR-FTIR data, analysis of XPS spectra, and a table of prepolymer properties. This material is available free of charge via the Internet at http://pubs.acs.org.

■ AUTHOR INFORMATION

Corresponding Author

ashby@email.unc.edu

Notes

The authors declare no competing financial interests.

■ ACKNOWLEDGMENTS

We would like to thank the DeSimone group for providing expertise and supplies for PRINT and cytotoxicity experiments, Dr. Carrie Donley of UNC CHANL for assistance with XPS, and Dr. Natalia Lebedeva for numerous helpful discussions and assistance with the shape memory movie. The ATR-FTIR measurements were performed in the UNC EFRC Instrumentation Facility funded by the UNC EFRC: Solar Fuels and Next Generation Photovoltaics, an Energy Frontier Research Center funded by the U.S. Department of Energy, Office of Science, Office of Basic Energy Sciences under Award Number DE-SC0001011 and by UNC SERC: "Solar Energy Research Center Instrumentation Facility" funded by the US Department of Energy, Office of Energy Efficiency & Renewable Energy under Award Number DE-EE0003188). Funding was provided from NSF DMR grants 0418499 and 1122483.

■ REFERENCES

(1) Assender, H.; Bliznyuk, V.; Porfyrakis, K. *Science* **2002**, *297*, 973−976.
(2) Autumn, K.; Liang, Y. A.; Hsieh, S. T.; Zesch, W.; Chan, W. P.; Kenny, T. W.; Fearing, R.; Full, R. J. *Nature* **2000**, *405*, 681−685.
(3) Gu, Z. Z.; Uetsuka, H.; Takahashi, K.; Nakajima, R.; Onishi, H.; Fujishima, A.; Sato, O. *Angew. Chem., Int. Ed.* **2003**, *42*, 894−897.
(4) Faucheux, N.; Schweiss, R.; Lützow, K.; Werner, C.; Groth, T. *Biomaterials* **2004**, *25*, 2721−2730.
(5) Sethuraman, A.; Han, M.; Kane, R. S.; Belfort, G. *Langmuir* **2004**, *20*, 7779−7788.
(6) Pierschbacher, M. D.; Ruoslahti, E. *Nature* **1984**, *309*, 30−33.
(7) Lendlein, A.; Langer, R. *Science* **2002**, *296*, 1673−1676.
(8) Yakacki, M. Y.; Shandas, R.; Lanning, C.; Rech, B.; Eckstein, A.; Gall, K. *Biomaterials* **2007**, *28*, 2255−2263.
(9) Sharp, A. A.; Panchawagh, H. V.; Ortega, A.; Artale, R.; Richardson-Burns, S.; Finch, D. S.; Gall, K.; Mahajan, R. L.; Restrepo, D. *J. Neural Eng.* **2006**, *3*, L23−L30.
(10) Nagase, K.; Kobayashi, J.; Okano, T. *J. R. Soc. Interface* **2009**, *6*, S293−S309.
(11) Hendrickson, G. R.; Lyon, L. A. *Soft Matter* **2009**, *5*, 29−35.
(12) Cole, M. A.; Voelcker, N. H.; Thissen, H.; Griesser, H. J. *Biomaterials* **2009**, *30*, 1827−1850.
(13) Alexander, C.; Shakesheff, K. M. *Adv. Mater.* **2006**, *18*, 3321−3328.
(14) Gil, S. E.; Hudson, S. M. *Prog. Polym. Sci.* **2004**, *29*, 1173−1222.
(15) Jeong, B.; Gutowska, A. *Trends Biotechnol.* **2002**, *20*, 305−311.
(16) Kuroki, H.; Tokarev, I.; Minko, S. *Annu. Rev. Mater. Res.* **2012**, *42*, 343−372.
(17) Miyata, T.; Uragami, T.; Nakamae, K. *Adv. Drug Delivery Rev.* **2002**, *54*, 79−78.
(18) Miyata, T.; Nakamae, K.; Hoffman, A.; Kanzaki, Y. *Macromol. Chem. Phys.* **1994**, *195*, 1111−1120.
(19) Chen, Y. H.; Chung, Y. C.; Wang, I. J.; Young, T. H. *Biomaterials* **2012**, *33*, 1336−1342.
(20) Chen, L.; Liu, M.; Bai, H.; Chen, P.; Xia, F.; Han, D.; Jiang, L. *J. Am. Chem. Soc.* **2009**, *131*, 10467−10472.
(21) Stuart, M. A. C.; Huck, W. T. S.; Genzer, J.; Muller, M.; Ober, C.; Stamm, M.; Sukhorukov, G. B.; Szleifer, I.; Tsukruk, V. V.; Urban, M.; Winnik, F.; Zauscher, S.; Luzinov, I.; Minko, S. *Nat. Mater.* **2010**, *9*, 101−113.
(22) Davis, K. A.; Burke, K. A.; Mather, P. T.; Henderson, J. H. *Biomaterials* **2011**, *32*, 2285−2293.

(23) Le, D. M.; Kulangara, K.; Alder, A. F.; Leong, K. W.; Ashby, V. S. *Adv. Mater.* **2011**, *23*, 3278−3283.
(24) Ebara, M.; Uto, Koichiro, U.; Idota, N.; Hoffman, J. M.; Aoyagi, T. *Adv. Mater.* **2011**, *24*, 273−278.
(25) DeForest, C. A.; Polizzotti, B. D.; Anseth, K. S. *Nat. Mater.* **2009**, *8*, 659−664.
(26) Haensch, C.; Hoeppener, S.; Schubert, U. *Nanotechnology* **2008**, *9*, 135302−135308.
(27) Prakash, S.; Karacar, M. B.; Banerjee, S. *Surf. Sci. Rep.* **2009**, *64*, 233−254.
(28) Zhang, Y.; He, H.; Gao, C.; Wu, J. *Langmuir* **2009**, *25*, 5814−5824.
(29) Rozkiewicz, D. I.; Gierlich, J.; Burley, G. A.; Gutsmiedl, K.; Carell, T.; Ravoo, B. J.; Reinhoudt, D. N. *ChemBioChem* **2007**, *8*, 1997−2002.
(30) Riva, R.; Schmeits, S.; Jérôme, C.; Jérôme, R.; Lecomte, P. *Macromolecules* **2007**, *40*, 796−803.
(31) Shibata, Y.; Tanaka, H.; Takasu, A.; Hayashi, Y. *Polym. J.* **2011**, *43*, 272−278.
(32) Naolou, T.; Busse, K.; Kressler, J. *Biomacromolecules* **2010**, *11*, 3660−3667.
(33) Zhu, Y.; Gao, C.; Lui, X.; Shen, J. *Biomacromolecules* **2002**, *3*, 1312−1319.
(34) Tretinnikov, O. N.; Ikada, Y. *Langmuir* **1994**, *10*, 1606−1614.
(35) Senshu, K.; Yamashita, S.; Mori, H.; Ito, M.; Hirao, A.; Nakahama, S. *Langmuir* **1999**, *15*, 1754−1762.
(36) Pike, J. K.; Wynne, K. J.; Ho, T. *Chem. Mater.* **1996**, *8*, 856−860.
(37) Baskin, J. M.; Prescher, J. A.; Laughlin, S. T.; Agard, N. J.; Chang, P. V.; Miller, I. A.; Lo, A.; Codelli, J. A.; Bertozzi, C. R. *Proc. Natl. Acad. Sci. U.S.A.* **2007**, *104*, 16793−16797.
(38) Gill, H. S.; Tinianow, J. N.; Ogasawara, A.; Flores, J. E.; Vanderbilt, A. N.; Raab, H.; Scheer, J. M.; Vandlen, R.; Williams, S. P.; Marik, J. *J. Med. Chem.* **2009**, *52*, 5816−5825.
(39) Pahimanolis, N.; Vesterinen, A. H.; Rich, J.; Seppala, J. *Carbohyd. Polym.* **2010**, *82*, 78−82.
(40) Wu, J.; Gao, C. *Macromol. Chem. Phys.* **2009**, *210*, 1697−1708.
(41) Wang, Y.; Betts, D. E.; Finlay, J. A.; Brewer, L.; Callow, M. E.; Callow, J. A.; Wendt, D. E.; DeSimone, J. M. *Macromolecules* **2011**, *44*, 878−885.